Electron-yield extended x-ray absorption fine structure with the use of a gas-flow electron detector

M. E. Kordesch and R. W. Hoffman
Department of Physics, Case Western Reserve University, Cleveland, Ohio 44106
(Received 6 September 1983)

We report the first electron-yield extended x-ray absorption fine-structure (EXAFS) measurements on a thick sample at ambient pressure using an ion chamber situated directly in the incident photon beam. An electron-detected EXAFS spectrum of an iron plate was acquired using a windowless, He-flow ion chamber at atmospheric pressure, thus extending the useful application of EXAFS to samples previously inaccessible by conventional techniques or not suited to ultrahigh vacuum environments.

Within recent years extended x-ray absorption fine-structure (EXAFS) analysis has become a useful technique to obtain structural information. In order to determine quantitative information for each coordination sphere, an equation for the absorption cross section must be obtained in terms of the observed spectral intensities. Electron-yield EXAFS is the nonradiative analog of x-ray fluorescence EXAFS and provides similar information; however, the electron-yield measurement is inherently surface sensitive since the electrons can only escape from the near-surface region of the sample. Electron EXAFS has been generally regarded as possible only in ultrahigh vacuum (UHV).[1,2] The method reported here extends the surface sensitivity available in EXAFS measurements to real environments and nonthin film samples, in particular, thick samples with surface layers composed of materials also present in the bulk substrate.

Detection of secondary electrons or fluorescent x-ray radiation emitted following a core-hole relaxation improves sensitivity through background suppression so that submonolayer quantities may be observed. For these cases, the ratio of the scattered-to-incident intensity may be written as[1]

$$\frac{I_s}{I_0}=\epsilon\frac{\Omega}{4\pi}\frac{\mu_x(E)}{\mu_x(E)+n(E)}(1-\exp\{-[\mu_x(E)+n(E)]x\}) \ ,$$

where I_s and I_0 are the intensity of the scattered and incident radiation, ϵ the quantum yield, $\Omega/4\pi$ the detector solid angle and efficiency, $\mu_x(E)$ the absorption coefficient for the sample through the tunable energy range of the x-ray radiation, and $n(E)$ the exponential attenuation of the nonradiative signal. In the fluorescence case, $n(E)$ is replaced by $\mu_x(E_f)$, the absorption coefficient evaluated at the characteristic fluorescence energy E_f.

For nonradiative detection, the equation for I_s/I_0 is easily solved for μ_x since the sample thickness is defined by the escape depth of the electrons. Conversion-electron Mössbauer spectroscopy (CEMS) results show that electrons with energies in the 5–7-keV range originate no more than 300 nm from the iron surface.[3] The escape depth for ion fluorescence radiation is several μm. Fluorescence detection is usually preferred to transmission EXAFS for thin samples less than a μm thick. For such samples, $\mu_x x$ is much less than one and the thin, single-component limit derived often in the literature is reached.[1,4,5] The greater attenuation of the electron-yield signal may be a significant advantage when thick (>1 μm) samples are concerned. When $\mu_x x$ is much greater than one, the solution of Eq. (1) for fluorescence detection is complicated by the contribution of the exponential term; at even greater thicknesses the exponential term approaches zero, and I_s/I_0 will approach a constant.

The inability of electrons to pass through windows necessitates enclosing the sample inside the detector. The detector design shown in Fig. 1 exploits the relative insensitivity of helium to the incident x-ray beam while efficiently counting the 5–6-keV (Ref. 6) Auger electrons. The detector-cell combination was a Lucite box made by gluing three 6-mm-thick plates together and milling out the appropriate spaces for the sample and detector. The overall dimensions of the detector-cell combination are $60\times56\times18$ mm and were chosen so that the cell would fit into our standard fluorescence chamber assembly.

The upper front half of the cell is removable for sample access and also contains the electron detector. The Lucite detector has a rectangular cavity milled in the center; the flat sides are lined with aluminum foil and two 0.01-mm-diam Au-coated W wires are stretched lengthwise on either side of the central slot that allows the beam to enter the counter. In this detector, the electrodes are not exposed to the incident beam in order to reduce scattering and background contributions. The cell is sealed on both sides with Kapton tape. Helium or 4% methane in helium gas is introduced through flexible tubing at about 0.1 ft^3/h at atmos-

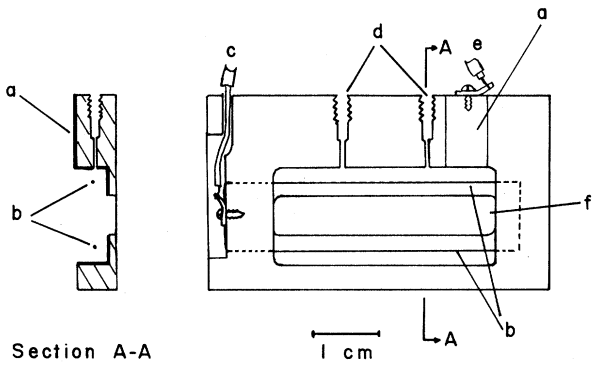

FIG. 1. View of the detector portion of the Lucite box, from the sample side: a, aluminum foil electrode covering the flat surface and side walls of the detector, with connection tab; b, Au-coated W wires; c, cable connection from electrometer to counter wires; d, gas inlet and outlet; e, bias connector to aluminum foil electrodes; f, detector window covered with Kapton tape.

pheric pressure. The aluminum foil electrodes are at −45 V with respect to the pair of gold wires. Currents are measured with an electrometer circuit that is also used for fluorescence measurements. At these low voltages the detector is a current chamber, and does not use field intensified ionization; although we have used similarly designed counters in CEMS with the central wires at +1200–1500 V.[7] Field intensified ionization was not necessary under the present experimental conditions, but offers a possible advantage in lower count-rate experiments.

Figure 2 shows the electron-yield EXAFS spectrum of a 1-mm-thick iron plate obtained on the focused beam line II-3 with use of Si(111) monochromator crystals at the Stanford Synchrotron Radiation Laboratory. The iron-edge electron-yield data are plotted as the ratio of the current in the electron detector to that in the incident ion chamber and are shown as curve A. For comparison, transmission data obtained from a 5-μm-thick Fe calibration foil are shown plotted in B on a $\ln I_0/I_T$ scale. The ordinates are therefore linear plots of the absorption coefficient on scales chosen to make the edge step approximately the same.

In order to verify that electrons were responsible for the signal observed in A, a piece of tape was placed over the face of the sample to block the electrons. This spectrum is shown in C. The most significant features of curve C are the greatly reduced signal and lack of EXAFS oscillations. There is an iron edge present, which we attribute to a residual sensitivity of the flow gas to backscattered x rays. The iron plate produces a substantial fluorescence signal that easily penetrates the tape, and subsequently passes through the electron detector where a small fraction is counted. In fact, examination of the incident photon signal, measured at the I_0 ion chamber upstream of the electron detector, indicates that some fluorescent x rays from the iron plate enter the I_0 chamber. Even though the curves shown in Fig. 2 are ratios of the electron-detector signal to I_0, the perturbation of I_0 by fluorescence radiation is apparent in curve C, and accounts for some of the structure visible above the iron edge. The absence of EXAFS oscillations is the result of a "thick limit" specimen.

Examination of the electron-yield data shows a signal to noise comparable with the optimized transmission case. The use of electron detection in order to provide an enhanced sensitivity is, of course, not new. However, a cell and detector design which allows detection of the high-energy Auger electrons with good signal to noise now makes possible the near-surface examination in a real environment. While it is necessary to enclose the sample inside the detector, placing the detector in the incident beam does not interfere with the electron-yield signal. In addition, the sample itself is independent of the detector circuit, allowing *in situ* experiments similar to those performed with CEMS[7] that are not possible with photocathode electron-detection schemes.[8] Finally, the detector materials are inert and inexpensive, making corrosion studies particularly attractive.

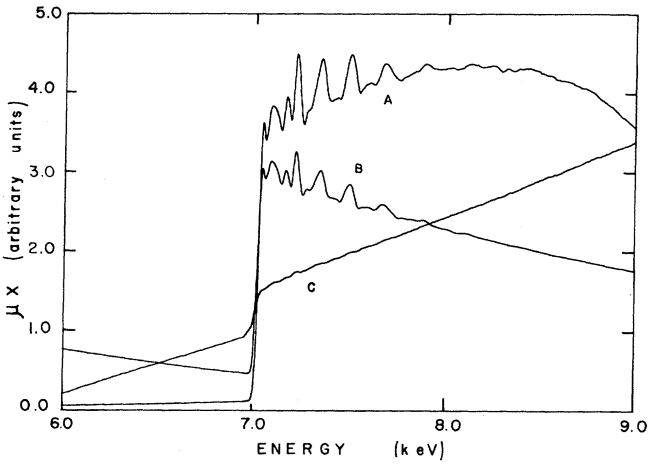

FIG. 2. Curve A, electron-yield EXAFS from an iron plate; curve B, transmission EXAFS from an iron foil; curve C, electron-yield EXAFS from same sample as A with tape covering surface.

ACKNOWLEDGMENTS

We would like to acknowledge helpful discussions with D. R. Sandstrom and F. W. Lytle. This research was supported by the Office of Naval Research under Grant No. N00014-79C-0795. The Stanford Synchrotron Radiation Laboratory is supported by the National Science Foundation and the U. S. Department of Energy.

[1]P. A. Lee, P. H. Citrin, P. Eisenberger, and B. M. Kincaid, Rev. Mod. Phys. 54, 769 (1981).
[2]J. Stohr, J. Vac. Sci. Technol. 16, 37 (1979).
[3]W. Jones, J. M. Thomas, R. K. Thorpe, and M. J. Tricker, Appl. Surf. Sci. 1, 388 (1978).
[4]J. Jaklevic, J. A. Kirby, M. P. Klein, A. S. Robertson, G. S. Brown, and P. Eisenberger, Solid State Commun. 23, 679 (1977).
[5]G. S. Brown and S. Doniach, in *Synchrotron Radiation Research,* edited by H. Winick and S. Doniach (Plenum, New York, 1980), pp. 353–386.
[6]D. A. Shirley, Phys. Rev. A 7, 1520 (1973).
[7]M. E. Kordesch, J. Eldridge, D. A. Scherson, and R. W. Hoffman, J. Electrochem. Soc., Ext. Abstr. 83-1, Abstract No. 55 (1983).
[8]N. J. Shevchik and D. A. Fischer, Rev. Sci. Instrum. 50, 577 (1979).